

Conf-420311-6

MAY

PPPL-CFP--2608

10th Plasma-Surface Interactions, submitted to J. Nucl. Mater (Apr, 1992)

DE92 012674

## Laboratory Studies of Spectroscopic Markers for the Characterization of Surface Erosion by Plasmas.

Dennis M. Manos, Timothy Bennett, Michele Herzer\*, and John Schwarzmann, Princeton University, Plasma Physics Laboratory, Princeton, NJ

\* visiting Research Associate, permanent address: Neshaminy High School, Langhorne, PA

### Abstract

The erosion rates in portions of fusion plasma devices like the ITER tokamak are sufficiently high that nearly real-time information on cumulative removal is needed for control and machine safety. We are developing a digitally- encoded scheme to indicate the depth of erosion at numerous poloidal and toroidal locations around ITER. The scheme uses materials embedded in the walls and divertors, which, when uncovered, present remotely detectable signals. This paper reports laboratory experiments on prototype markers consisting of combinations of up to 5 elements (Au,Pd,Ag,In,Ga) along with Au,Pt, and Ta pure metals. The markers were bonded to 4-D carbon-carbon composite of the type proposed for use in the ITER first wall, and placed in the the lower-hybrid-driven plasma of the atomic beam facility at PPL. The paper describes this device Light emission was characterized using a 1 meter Czerny-Turner vacuum ultraviolet monochromator. The samples were characterized both before and after plasma exposure by Auger spectroscopy.

We report the time-dependent behavior of the spectra of the visible and ultraviolet light emitted by the plasma when the markers are uncovered by the erosion showing emission lines of the marker elements which are easily distinguished from the background plasma lines. The dependence of the light intensity on bias voltage is compared to the known sputtering yields of the elements. The optical detection method allows exploration of the threshold dependence of these multi-element targets. An exponential dependence of yield above threshold was observed for all of the elements studied.

### 1.) Introduction

Erosion and redeposition of the divertor and first walls are among the major technical concerns of the ITER project [1]. Previously, we proposed a scheme to monitor erosion at a large number of places around the ITER tokamak[2]. The scheme is based on the implantation of various "markers" of suitably selected elements placed at specified depths, poloidal, and toroidal locations. These markers, when exposed as a result of erosion, are intended to sputter these elements into the plasma where electron impact processes will excite radiative optical transitions. Quantitative measurement of such emission is likely to be difficult because of the large differences in sputtering, evaporation, and radiative excitation cross-sections for materials which are suitable for use as markers. Thus we proposed the use of a scheme where, only the qualitative presence of a

**MASTER**

EB

marker material, above a determined background, will serve to identify the state of the first wall or divertors.

The scheme identifies locations by assigning them binary numbers. The basis set for the bits of the binary number consists of spectroscopic lines associated with each of the elements in the marker set. For example, a marker set may be formed from three elements: Au, Ag, and Pd. The presence of Pd could assign a 1 for the  $2^0$  bit, its absence then would assign a 0 to the  $2^0$  bit. Similarly Ag could assign the  $2^1$  place and Au the  $2^2$  place. With this set, one could encode 7 locations (ranging from 001 [Pd only] to 111 [Pd, Ag, and Au]), provided that no markers overlapped in time, or allowing for deconvolution of overlapping markers (a less desirable scenario). To avoid overlapping, markers must release material for only a brief period of time and marker elements must not recycle above the background offset in the detection system. Current experience from both impurity injection and from accidental release of materials from probes, is that such elements do not reappear in successive discharges after the source is removed.[3] A set of  $n$  such elements allows one to encode  $2^n - 1$  locations. For ITER, a set of 10 to 13 such elements, given other limitations on the method, are sufficient to encode up to several thousand locations.

In addition, there are other requirements for a marker set. Foremost is the ability to discriminate unambiguously between spectroscopic lines of 10 or more trace elements simultaneously. This requires high resolving power in detection, since emission lines of most suitable elements are quite numerous. The metallurgical preparation or beam implantation of such markers also represents a formidable challenge. The exposed area of some markers may have to cover many square centimeters to guarantee detectability. The zones of greatest interest are also those subjected to the highest heat flux. The presence of implanted markers must not seriously degrade the performance of the wall material. Means by which such a marker can be employed must be devised.

It is also important to characterize the temporal behavior of the spectroscopic signals from multi-element materials. For improper choices of marker, more volatile components, or those with higher sputtering yields, may disappear too soon, making marker location assignments difficult. The present state of understanding of multi-component sputtering is insufficient for design of such

a system [4]. The high recycling mode of operation proposed for ITER will produce low electron temperatures in the scrape-off in an attempt to stay below the sputtering threshold, thus allowing the possible use of high-Z refractory materials for power handling[5]. In this work therefore, we have made measurements at low ion energy, exploiting the sensitive detection of optical spectroscopy [6] to determine accurately the observed location of threshold energies, since these may differ from those of the pure elements in some alloys or mixtures.

## 2.) Apparatus and Method

The apparatus, which has been described in detail in earlier publications [7], is shown in Figure 1. A lower-hybrid-wave driven coaxial source [8], contained in a 3-5 kG solenoidal magnetic field, is powered by a 1kW, pulsed (10Hz), microwave source at 2.45 GHz. The plasma streams to a limiter plate which can be d.c. biased from +75 to -600 volts, though, in practice, bias voltages more positive than -5 volts frequently result in unstable plasma operation and are not used. Gas is pulsed (10Hz) directly into the coaxial source outer cup through a Veeco PV-10 valve. The steady state He pressure in the limiter chamber rises to approximately 20 mtorr. The pulse widths and delays are adjusted for optimal coupling to give the highest fluence on target without overheating the target and source. Figure 2 shows operating waveforms for a typical He plasma. The ion current is 3- 5 amperes, yielding 3-5 amps/cm<sup>2</sup> on the limiter during the pulse. Plasma densities and temperatures have been measured with Langmuir probes. The value of the  $n_e$  on axis depends on gas species and power, varying from a few times  $10^{12}$  cm<sup>-3</sup> at low power in He, up to  $8 \times 10^{13}$  cm<sup>-3</sup> at 1 kW in Ar. The radial profile of the density is approximately triangular, with a full width at half maximum of approximately 1 cm., independent of working gas.  $T_e$  varies from 5 to 10 eV, and is almost flat across the density profile. For the He discharges used in this work,  $n_e(0) = 1 \times 10^{13}$  cm<sup>-3</sup>,  $T_e(0) = 5.5$  eV, and  $V_s = 15$  eV.  $V_s$  is obtained by adding the appropriate  $T_e$ -dependent sheath potential to the measurement of the floating potential [9].

In some studies, samples were bonded to tantalum limiter plates. Tantalum was selected for its high energy threshold and low yield on He bombardment, representing a prototype refractory first-wall material. In other studies, carbon tile materials, similar to those used on the first wall of TFTR were used. Markers were embedded under the surface of such tiles, using

graphite glue to bond them. Markers also were bonded to the flat front surface of carbon-tile limiters and a thin, pyrolytic carbon overlayer was applied using a method developed for suppression of multipactoring on high-power microwave waveguides [10].

The use of optical methods for the determination of sputtering yields is well-established [6]. Visible and ultraviolet radiation from the zone a few mm. above the target plate was collected by a 1 m Czerny-Turner, VUV spectrometer, fitted with a 2400 line/mm grating, and an RCA 4837 photomultiplier tube (PMT), having a bialkali photocathode. The pre-amplified signal from the PMT passed to a PAR Model 162/164 boxcar integrator. The (stationary) gate-width of the boxcar was adjusted to fall within the microwave pulse (see Fig 2b). The boxcar output was low-pass filtered and recorded on a single channel strip chart.

Auger spectroscopy was used to characterize the surface composition of multi-element markers. Various elemental materials and combinations were assessed. We will restrict this paper to a representative case of a particular alloy with a nominal bulk composition of 45% Au, 40.5% Pd, 5.0% Ag, ~5% In, and the remainder primarily Ga with trace amounts of other metals. The several individual markers made from this alloy will be referred to as "marker D" throughout the remainder of this paper.

### **3.) Experimental Results**

Auger survey spectra of the surface of marker D before and after plasma exposure were taken. As seen in Figure 3a and 3c, adventitious impurities (S, Cl, C, and O), resulting from air transfer are detected on the surface. These were removed by pre-sputtering in our emission experiments, so to determine the resulting surface concentrations [11] presented to the plasma, we removed a layer ~25 angstroms thick and repeated the Auger analysis (Figs. 3b and 3d). Since the sensitivity factors for pure elements do not generally represent those of alloys, the percentages below cannot be regarded as quantitatively accurate. Changes in these percentages from plasma exposure may result either from alteration of the composition by preferential sputtering or changes in the nature of the binding resulting in changes in Auger sensitivity. We assume the former for the purpose of this discussion.

Plasma exposure increased the surface concentration of gold from 18% to 34%, and indium from 7.5% to 10.6%, while decreasing Ga from 13.4% to 4.6%. Pd and silver change only slightly due to plasma exposure. Iron and copper, which are probably residual surface

impurities associated with the rolling and forming operations, entirely removed by the plasma exposure. Scanning electron micrographs show that, over plasma exposed regions of the marker, approximately spherical spicules 0.05  $\mu\text{m}$  to 0.125  $\mu\text{m}$  in diameter are present. The 1.5% -3% duty cycle of the plasma was chosen so as not to overheat the surface of the marker. The unexposed markers have no asperities of this diameter, so it seems unlikely that these have resulted from surface melting. We hypothesize that these features are precipitations of material from composition changes during sputtering. In future work, Auger maps at high magnification will be used to determine the composition of these microscopic features.

Figure 4 shows an optical spectrum of a He plasma on a Ta limiter plate at a bias potential of -5 volts. The overlay lines indicate where neutral or singly ionized emission lines may be expected to be seen for candidate marker materials, including those present in marker D. Scans over large regions of wavelength were performed using marker D at various negative voltages to identify the strongest lines. Figure 5 illustrates that even at low gain elemental lines can be identified, not only by wavelength, but by their behavior with impinging ion energy. The He lines are unaffected by the change from -50 volts to -75 volts, whereas lines associated with the Ag and Pd increased dramatically in intensity.

To assess the behavior of the emission intensity as a function of impingement energy, the spectrometer wavelength is centered on the brightest lines of the elements in marker D, and the light intensity is recorded while changing the bias voltage. For comparison of the derived thresholds, we also repeated this procedure using pure elements bonded to the limiter.

Kreye [12] has analyzed this method in detail; his work indicates that emission intensity is a good measure of the sputtered atom density. To assess the quantitative sputtering rate from such measures requires taking into account the velocity of the sputtered species. Stuart, et. al. [13] found that the velocity distributions of ejected material, at least for  $\text{Ar}^+$  and  $\text{Kr}^+$  bombardment, varied with mass only over a factor of two at most, even for large changes in target mass (Be to Ag). Not correcting for the velocity dependence with ion bombardment energy is expected to produce only a small error; the relative intensity should be regarded as an upper bound for the sputtering yield as the energy is reduced. This should make the approach to a constant background level more indicative of the location of the threshold, rather than less, however. The results of our studies are shown in Figure 6.

In an ITER marker it will be highly desirable for the line radiation intensity to rise rapidly as the wall material erodes to uncover it, and to fall rapidly as the marker burns out. Such sharp transitions are analogous to “endpoint detection” methods common in semiconductor etching [14]. Figure 7 shows the onset of Pd line radiation from a 1 cm<sup>2</sup> lozenge of marker D covered by a 16μ thick layer of pyrolytic carbon, subjected to 3.5 amps/cm<sup>2</sup> at a bias voltage of -51 volts. The variability in intensity is beyond the noise of the detection system, indicating that the underlying layer is exposed in a non-uniform manner. Perhaps as the layer thins pinholes open and close exposing small amounts of the marker for periods of time. We observed a pronounced tendency toward unipolar arcing in these studies, particularly as the carbon layer just begins to clear or whenever the bias voltage is quickly set to values below - 50 volts. This is consistent with pinholes opening to constrict the discharge and overheat the interface layer between the metal and the carbon. Arcing may be a problem for such markers in ITER; special attention will have to be paid to methods by which they are embedded in the first wall.

#### 4.) Discussion

The threshold for sputtering of gold by Ar<sup>+</sup> was measured previously and found to be 17 eV for the (110) plane of a crystalline specimen [12]. As seen in figure 6, our observed threshold for He<sup>+</sup> is 30 volts (15 volts bias + Vs) for pure gold, is 35.5 volts for sputtering gold from the marker. Indium has a threshold at about 35 eV in the marker. Ga, Pd, and Ag appear to have thresholds below the lower limit we explored in this study, i.e., less than 15-17 volts. Ta and Pt (not shown) have thresholds of 43 and 40 volts respectively. Table 1 summarizes these observations .

Anderson and Bay [15] have suggested that threshold energies can be rationalized according to the following equations:

$$E_{th}/U_0 = 8(M_2/M_1)^{-1/3} \text{ for } M_2/M_1 < 3$$

$$E_{th}/U_0 = \gamma^{-1}(1-\gamma)^{-1} \text{ for } M_2/M_1 > 3$$

where  $U_0$  is the surface binding energy (assumed to be equal to the sublimation energy by those authors)  $M_1$  is the projectile mass,  $M_2$  is the target mass, and

$\gamma = 4 M_1 M_2 / (M_1 + M_2)^2$  is the energy transfer factor (0.078 for He<sup>+</sup> on Au, 0.561 for Ar<sup>+</sup> on Au). Straightforward application of these expressions to our results for He<sup>+</sup> on gold yield a surface binding energy of gold in marker D of 4.50 eV, compared to 3.82 eV in pure gold. However, using the literature value of 17 eV for argon, these expression predict a value of 58 eV for the threshold of He<sup>+</sup> on gold. This is in good agreement with the value of 55 eV given by Bay, Roth, and Bohdanský [16] for He<sup>+</sup> on Au, obtained by linear extrapolation of measured data above 170 eV. Those authors point out that linear extrapolation over such a distance is fairly uncertain. Their value is very much higher than our observed value of 30 eV, which, as can be seen from Figure 6, is uncertain by at most 5 volts. We will return to the subject of linear extrapolation below.

A complete discussion of sputtering near threshold has been given in Anderson and Bay [15]. We summarize only a few of their points here. Stuart and Wehner [6], who compared yields using Ne<sup>+</sup>, Ar<sup>+</sup>, Kr<sup>+</sup>, Xe<sup>+</sup>, and Hg<sup>+</sup> as projectiles, concluded that the energy transfer factor (mass ratio) played no significant role in determining the threshold value. Those authors found that the threshold value was approximately 4 times the sublimation energy of the target, independent of projectile mass. Our observed threshold for He on Ta, 43 eV, agrees with their threshold for Ar<sup>+</sup> on Ta measured. Though this finding supports their conclusion that the threshold behavior is independent of projectile mass, our results for He<sup>+</sup> on Au suggest that the effect of projectile mass is important, though much less pronounced than the equations of Anderson and Bay predict.

Although Stuart and Wehner address experimental problems of Hg contamination, and doubly ionized species in their studies, they do not discuss the possible cross-contamination caused by the possible persistence of the inert gases in their chamber implanted or co-deposited by prior discharges. Recent work has shown that such gases are quite persistent in some materials [17]. In the studies of the present paper, the base pressure of the apparatus was approximately  $1 \times 10^{-7}$  torr, consisting mainly of water, almost 5 orders of magnitude below the He pressure in these experiments. The limiters were not exposed to any other recycling gases, thus contamination by heavier gaseous species was probably not a problem. Though neutral carbon was present in

our discharge, the mean free path for ionization is too long for much of it to be ionized in the narrow, strongly magnetically confined discharge zone. Visible and ultraviolet surveys indicate that doubly ionized He is not present in our discharge at low limiter bias voltages.

The linear extrapolation of sputtering yields to determine thresholds has been discussed by Hotston [18], who, based on theoretical grounds, suggested that the procedure should be reasonable. For every material we investigated, the He<sup>+</sup> sputtering yield is very well represented by the form:

$$Y(E) = 0, \quad E \leq E_{th}$$

$$Y(E) = Y_0 \exp(E/E_k) \quad E > E_{th}, \text{ where } E_k \text{ is a fitting}$$

constant. We note that the exponential dependence persists out to 60-100 volts, which is as far as we pursued these measurements. Interestingly, for Pd, there is an abrupt transition from exponential behavior to linear behavior at an ion energy of 65 volts. The ion temperature in our plasma has been previously estimated to be ~0.5 eV [7]; thus the exponential dependence is not the result of convoluting a Maxwellian ion energy distribution at threshold. Table 1 lists the best fit values of the observed value of E<sub>k</sub>, the lower limit of the fitted energy range, E<sub>high</sub> the upper limit of the range, E<sub>th</sub>, the threshold energy, and the R-factor of the fit.

Table 1  
Fitting constants of the exponential yield function for projectile ion energy above threshold  
 $Y = Y_0 \exp(E/E_k)$  over the range E<sub>th</sub> to E<sub>high</sub>

Material	$\lambda$	E <sub>k</sub>	E <sub>high</sub>	E <sub>th</sub>	R
Ag, marker D	3280.68	21	70	n.o.	0.990
In, "	4511.32	26	105	35	0.999
Ga "	4172.06	21	95	n.o.	0.998
Au "	4792.60	9	85	35	0.987
Au, pure	4792.60	22	75	30	0.965
Pd, marker D	3634.69	21	75*	n.o.	0.994
Pd, "	3404.58	20	65*	n.o.	0.981
Ta, pure	5997.23	30	120	40	0.998

notes: n.o. means not observed \* Pd dependence becomes abruptly linear above 75 eV

The above findings indicate that a linear extrapolation for the determination of threshold energies is not generally valid. The observed thresholds, or lack thereof, are consistent with complicated

dynamic interactions for light ions at low energies previously suggested by other authors [19]

## 5.) Conclusions

This paper has shown that a spectroscopic marker system for use in the first wall of ITER, appears to be scientifically feasible. Some problems may be anticipated based on this work which require additional development effort to overcome. Arcing may occur as the first-wall overlayer on the marker becomes thin due to erosion. This can give somewhat premature indications of erosion to marker depth, and more importantly may cause uncontrolled amounts of high-Z impurity to enter the plasma. Better methods of implanting very thin markers must be used so that the temporal signature of markers will be sharp enough to permit the encoding a larger number of locations without providing for subtraction of overlaps. This work has also examined the behavior of a particular composite material for light ion sputtering near threshold. The observed behavior is not in accord with empirical rules for prediction of threshold locations, or the dependence of yield on projectile energy. This suggests that a number of individual marker compositions that are proposed for use in ITER would have to be evaluated in a high-density, low-temperature plasma environment such as the edge of TFTR, JET, or D-IIID, or perhaps in linear tokamak edge simulators [20], to provide a rational basis for design.

**Acknowledgements:** The authors wish to thank Richard Moore of Evans East, Inc., in Plainsboro, NJ, for performing the Auger and SEM analysis. We are grateful to the ITER project and to the Department of Energy for support of this work under contract DE-AC02-76CHO-3073.

## Figure Captions

Figure 1. Schematic diagram of the hyperthermal neutral beam apparatus. For these experiments, the limiter plate was rotated normal to the impinging plasma, so that markers mounted to it could be bombarded at normal incidence.

Figure 2. a) operating waveforms showing the microwave trigger pulse (top), the limiter ion current, for a limiter bias of -40 volts, and the end of the gas valve pulse (bottom). b) PMT output for a Pd line exposed to the plasma (top) and boxcar gate window (bottom)

Figure 3. Auger survey spectra of unexposed marker D (a) and (b) and plasma exposed marker D (c) and (d). The sputter clean was done to remove the adventitious layer associated with air handling. The concentrations observed for cleaned unexposed and exposed markers are as follows:

Unexposed:	Au 18%, Cu 4%, Pd 45%, Ag 2.6%, In 7.5%, Fe 5.6%, and Ga 13.4%
Exposed :	Au 34%, Cu 0%, Pd 38%, Ag 2.6%, In 10.6%, Fe 0%, and Ga 4.6%

See the text for caveats on the interpretation of these numbers.

Figure 4. Spectrum of He discharge taken at -5 volts limiter bias, where no metal emission lines of comparable intensity are produced. The location of marker candidate lines is indicated.

Figure 5. Comparison of emission observed using markers of Ag and Pd at bias voltages of -50 volts and -75 volts. The gain of the detector deliberately has been kept low to indicate the ease of contrasting background emission from metallic lines.

Figure 6. Emission intensities, assumed to be proportional to sputtering yields, as functions of bias voltage for 6 various marker elements. The wavelengths at which the data were taken are those listed in Table 1. The ion impingement energy is the difference of the bias voltage minus the plasma potential which was measured to be +15 volts. The background intensity at each wavelength has

not been subtracted. Where the intensity abruptly rises above background with increasing bias we presume a threshold for sputtering exists.

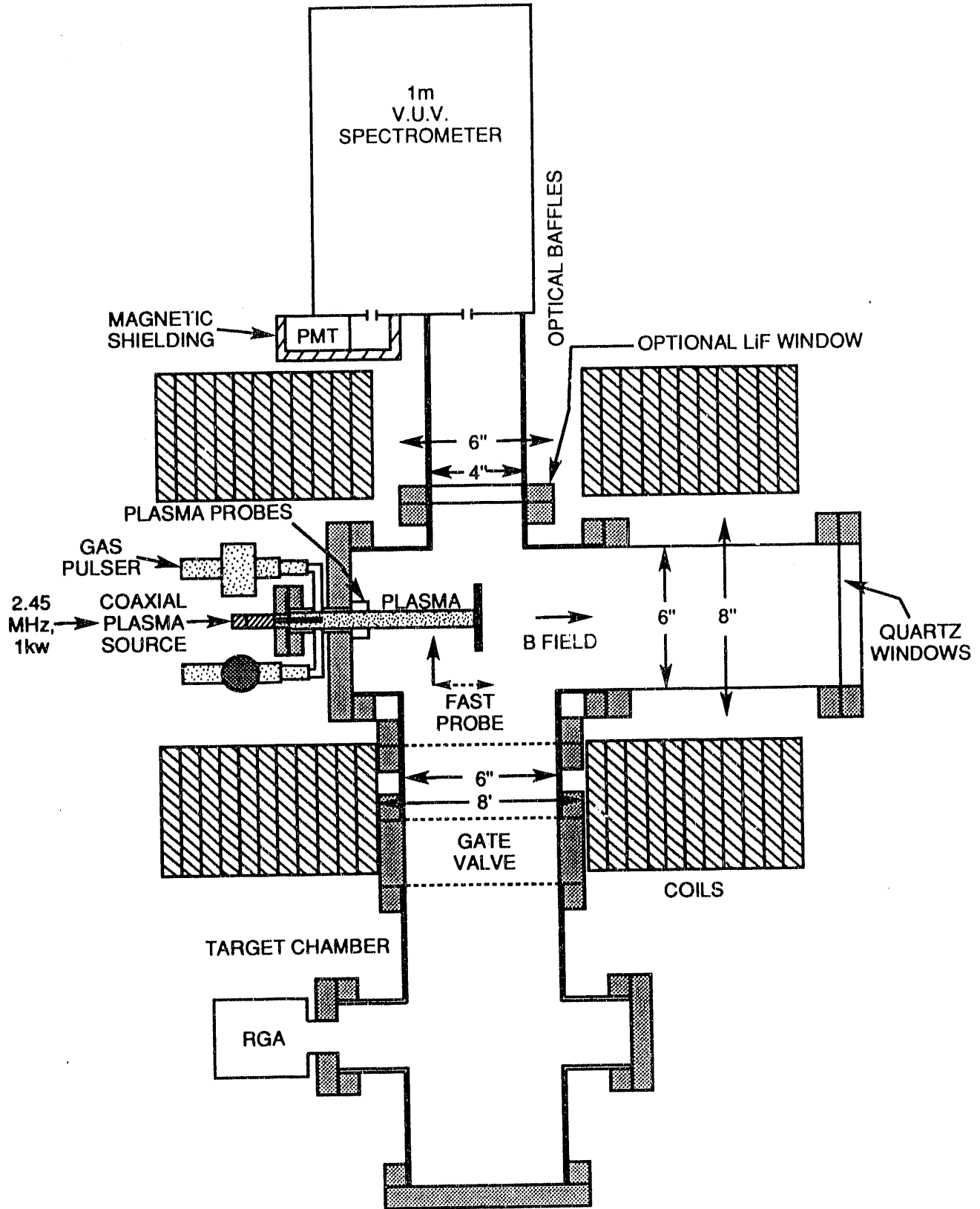
Figure 7. Temporal dependence of Pd line emission as a  $16\mu$  pyrolytic carbon film is eroded by plasma bombardment. The variation prior to the rapid increase is beyond the noise in the detection system, suggesting a non-uniform clearing of the film (see text)

## References

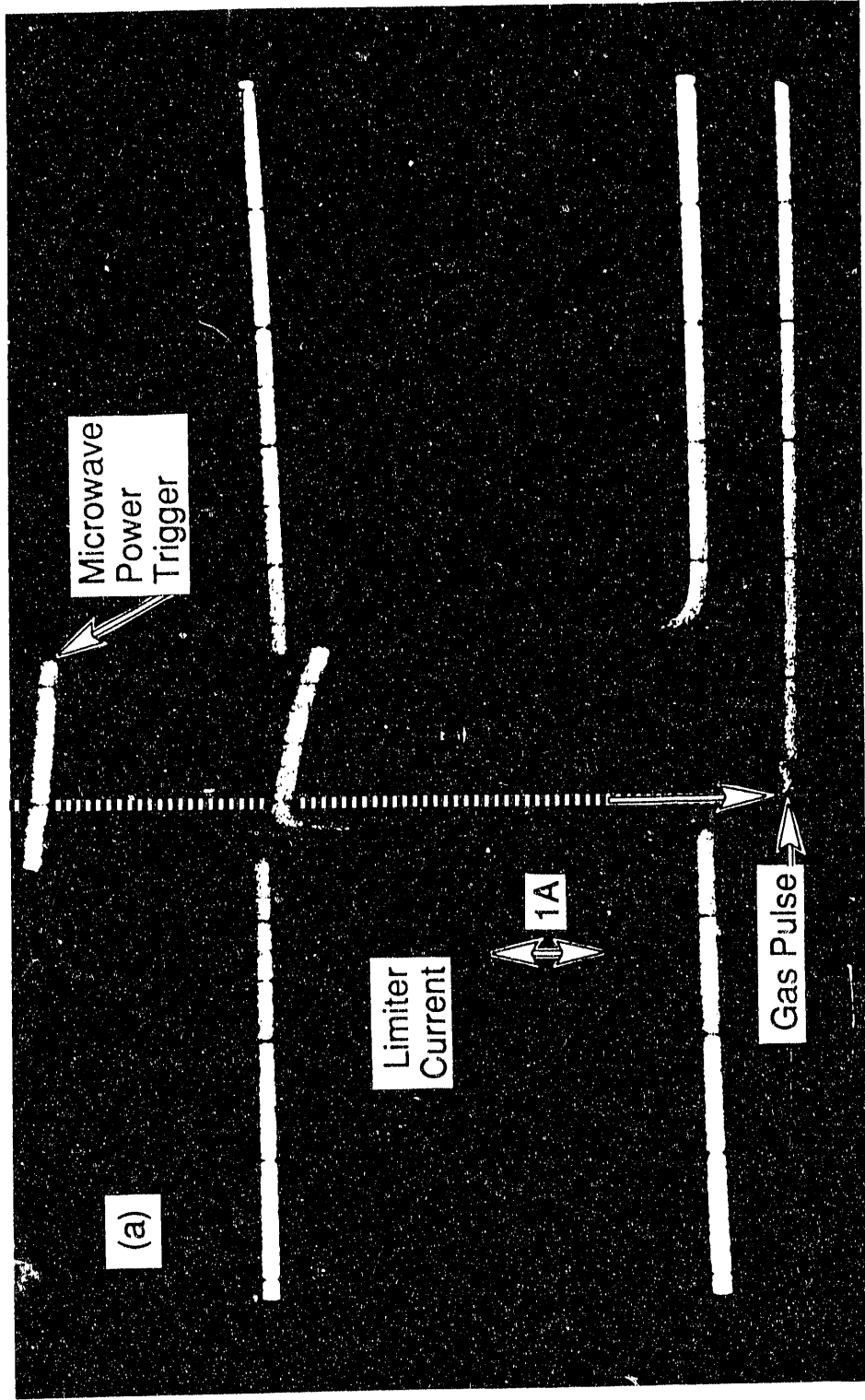
- [1] S. A. Cohen, K. A. Werley, PMI Issues for ITER, PPPL-2823 (February, 1992).
- [2] (a) D. M. Manos in ITER Diagnostics, Eds. V. Mukhovatov, K. M. Young, SA. Yamamoto, ITER Documentation Series No. 33, (IAEA, Vienna, 1990), p. 71.  
(b) K. M. Young, K. W. Hill, D. M. Manos, and G. Schilling, Bull. Am. Phys. 36 (1991) 2276.
- [3] B.C. Stratton, R.J. Hulse, A.T. Ramsey, J. Timberlake, P.C. Efthimion, E.D. Frederickson, B. Grek, K.W. Hill, D.W. Johnson, D.K. Mansfield, H. Park, F.J. Stauffer, G. Taylor, Nucl. Fus., 29, 437, (19
- [4] G. Betz and G. K. Wehner, Chapter 2 in "Sputtering by Particle Bombardment, Vol. II", Ed. R. Behrisch, (Springer-Verlag, Berlin, 1983), p. 11.
- [5] T Kuroda, G. Vieder, M. Akiba, A. B. Antipenkov, M. Araki, C. Bake, V. Barabash, Y. Blinov, J. Boutard, J. Brooks, A. Cardella, R. Causey, S. Chiochio, S. Cohen, P. Deschamps, A. Epinatjev, G. Federici, Y Gohasr., P. Goranson, A. Hassanein, P. Hubert, R Jakeman, J Koski, Y. Kuzmin, M Lipa, S Majumdar, R. Mattas, I. Mazul, Y. Prokofiev, V Renda, G. Shatalov, R Shaw, D. Smith, Y. Stebkov, H. Takatsu, V. Tanchuk, L. Tpiiskii, J. Van der Laan, R Watson, C Wu, E. Zolti, Iter Plasma Facing Components, Iter Doc Series 30, IAEA, Vienna, (1991)
- [6] R. V. Stuart and G. K. Wehner, J. Appl. Phys. 33 (1962) 2345.
- [7] (a) J. W. Cuthbertson, "Reflection of Plasma Ions from Metals", Ph.D. Thesis, Princeton University, (October, 1991), 201 pgs. Available from University Micro films, Ann Arbor, Michigan.
- [8] R. W. Motley, S. Bernabei and W. Hooke, Rev. Sci. Instrum. 50 (1979) 1586.
- [9] G. Chiu and S. A. Cohen, this volume
- [10] J. Timberlake, S.A. Cohen, C. Crider, G. Estep, W. Hooke, D.M. Manos, R. Moore, J. E. Stevens, and M. Ulrickson, J. Vac. Sci. Technol. 20, 1309 (1982)
- [11] Handbook of Auger Spectroscopy, 2nd Ed., L. E. Davis, N. C. MacDonald, P.W. Palmberg, G. E. Riach, R. E. Weber, PHI, Inc., (Flying Cloud Dr., Eden Prairie,

MN 55343).

- [12] W. C. Kreye, J. Appl. Phys. 35 (1964) 3575.
- [13] R. V. Stuart, G. K. Wehner, and G. S. Anderson, J. Appl. 40 (1969) 803.
- [14] D. M. Manos, and H. F. Dylla, Diagnostics of Plasma for Material Processing, Chapter 4, "Plasma Etching", Eds., D. M. Manos, and D. L. Flamm, (Academic Press, NY, 1989), p. 259.
- [15] H. H. Anderson and H. L. Bay, Chapter 4 in Sputtering by Particle Bombardment, Vol. I, Ed., R. Behrisch, (Springer-Verlag, Berlin, 1981), p 145.
- [16] H. L. Bay, J. Roth, and J. Bohdansky, J. Appl. Phys., 48 (1977) 4722.
- [17] A. T. Ramsey and D. M. Manos, this volume
- [18] E. Hotston, Nucl. Fus. 15 (1975) 544.
- [19] P. Behrisch, G. Maderlechner, BMU Scherzer, M.T. Robinson, Appl. Phys. 18 (1979) 391.
- [20] S.A. Cohen, "The ITER Divertor Experiment and Laboratory", to appear in Fusion Technology, (1992)



LOW ENERGY NEUTRAL BEAM SOURCE



1000

Photomultiplier  
Signal  
(Amplified)

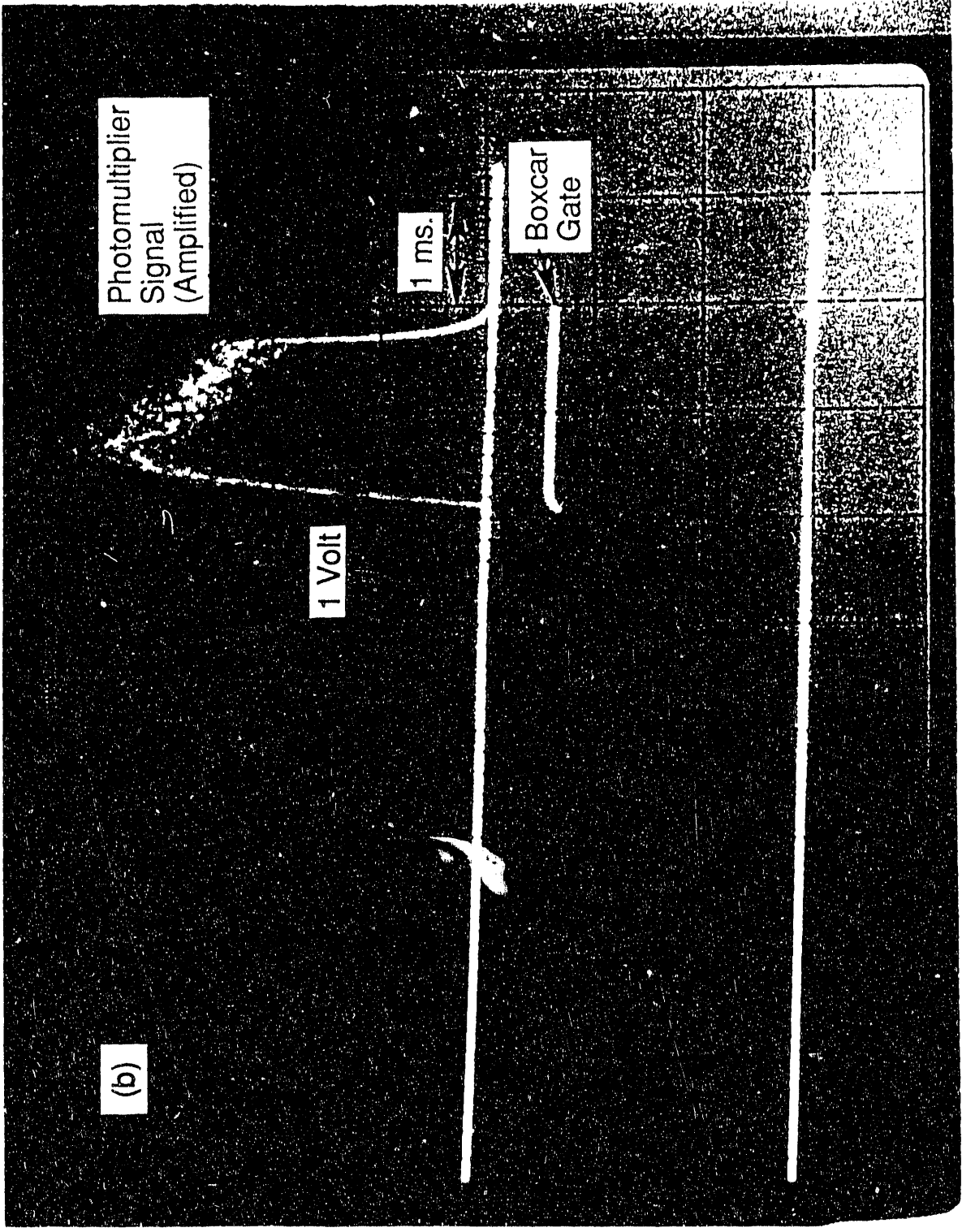
1 ms.

Boxcar  
Gate

1 Volt

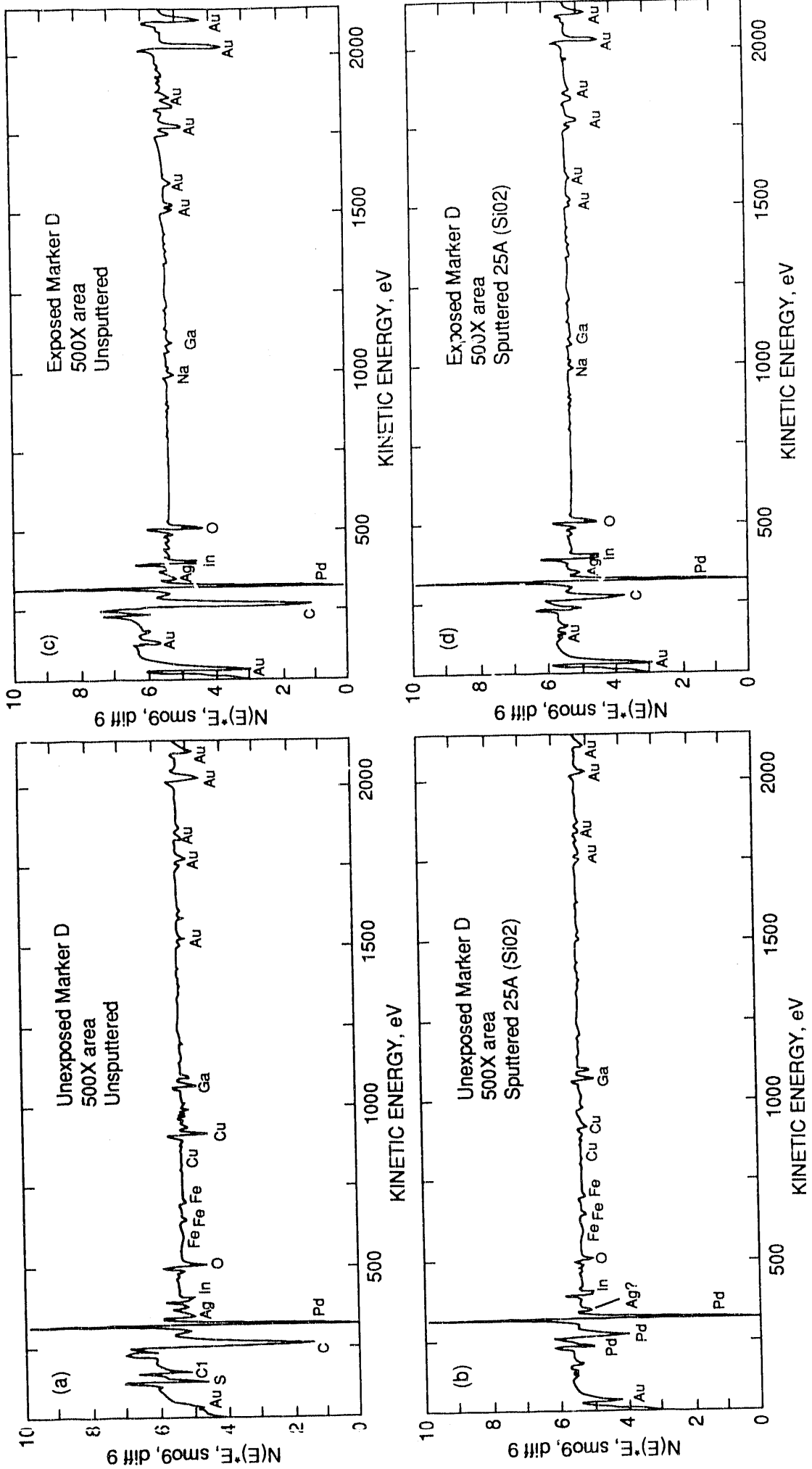
(b)

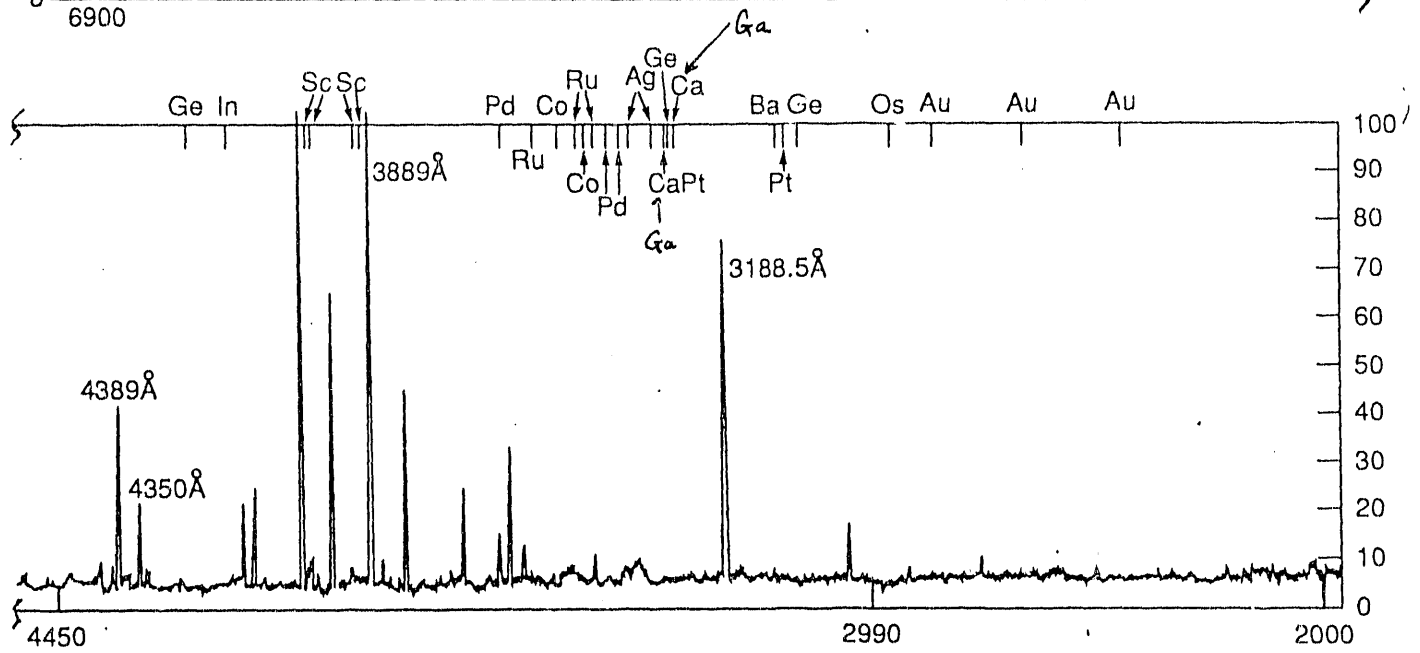
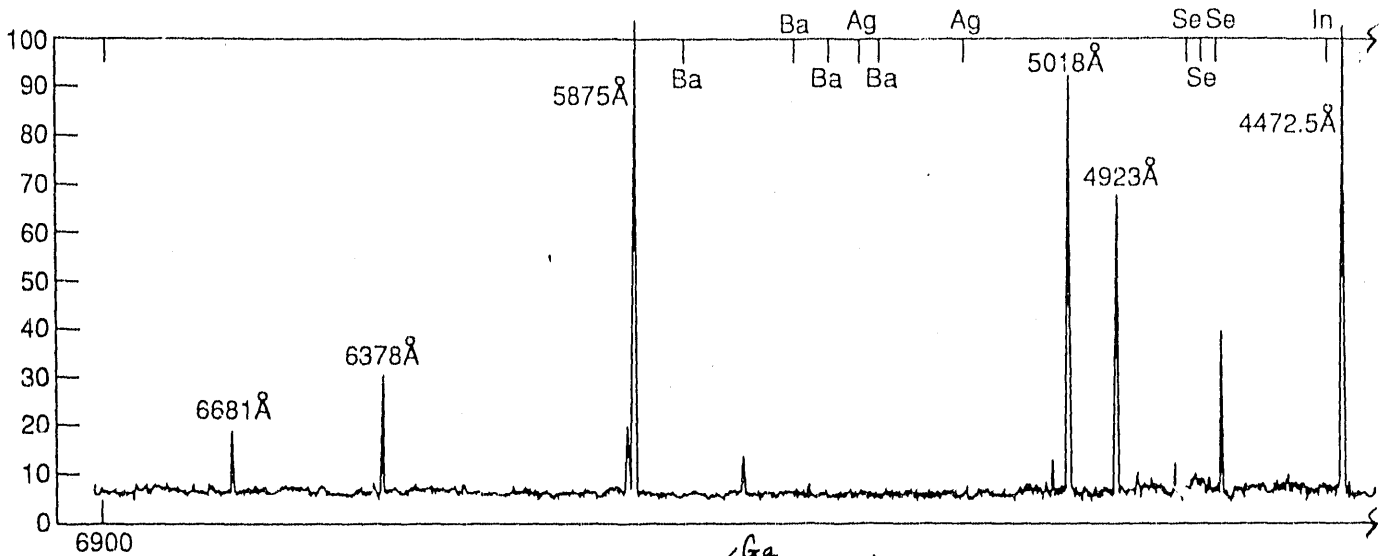
Fig. 2.107



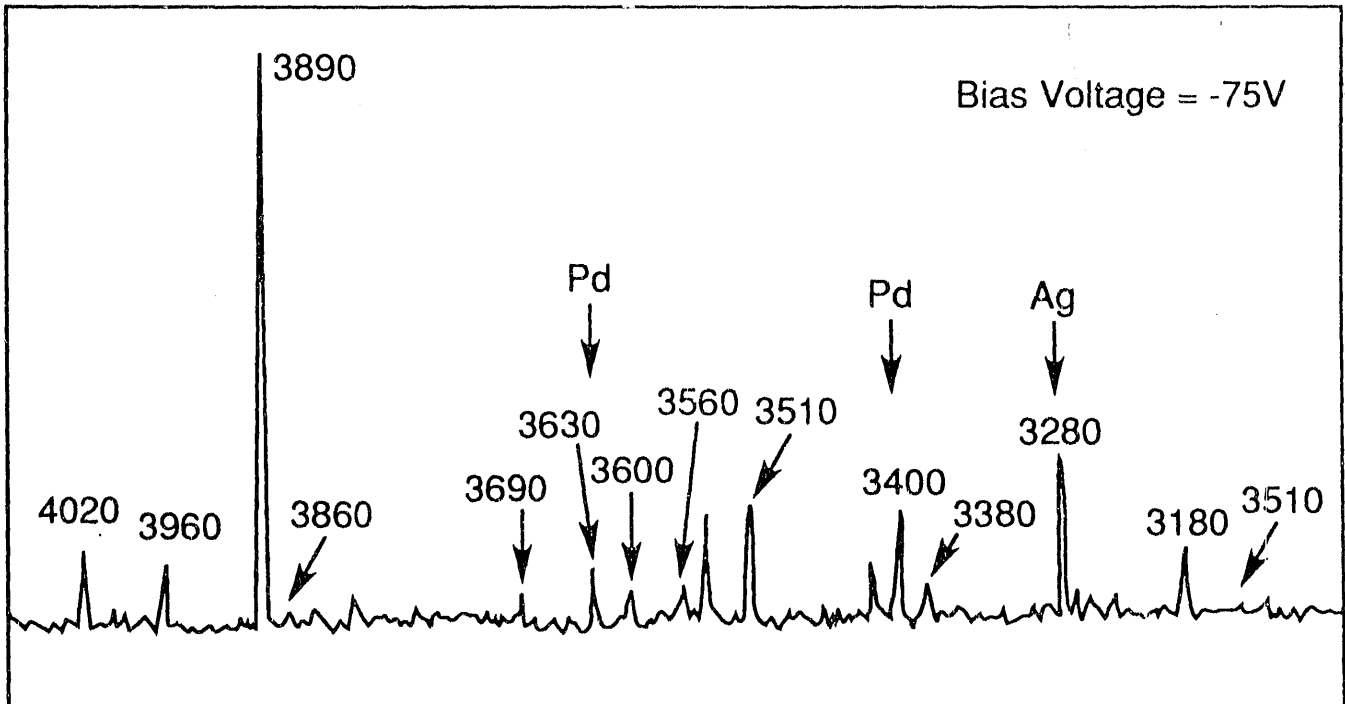
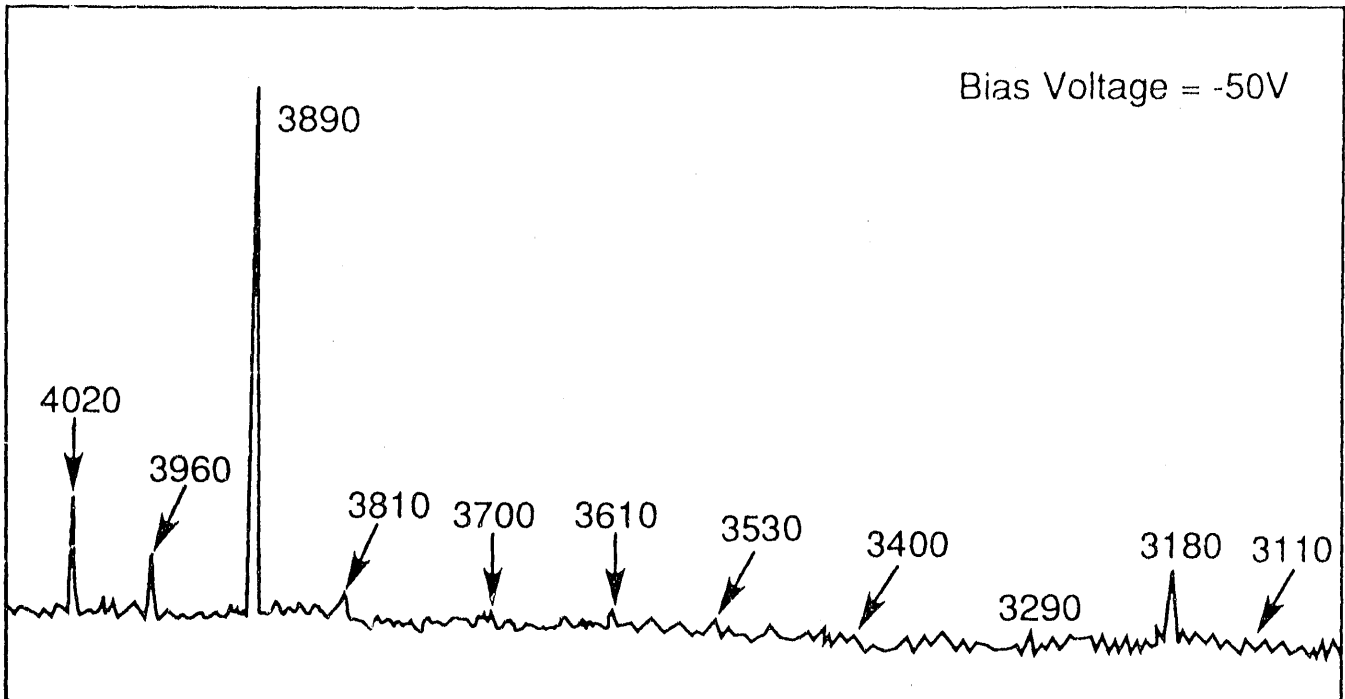
Manos et al  
10th PSI  
FIG 3

PPPL#92X0098

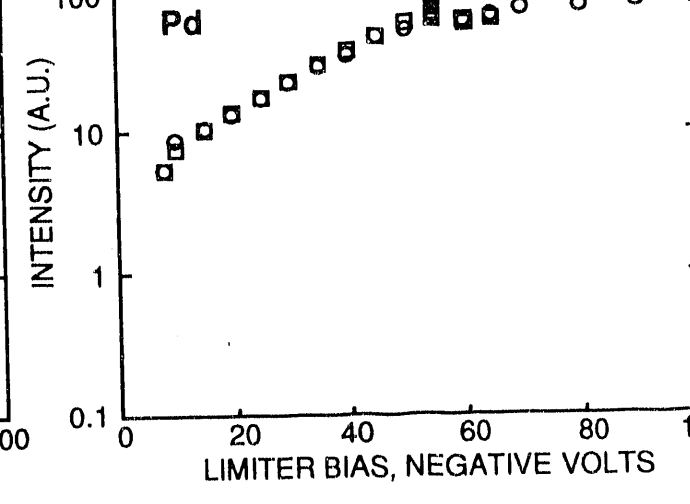
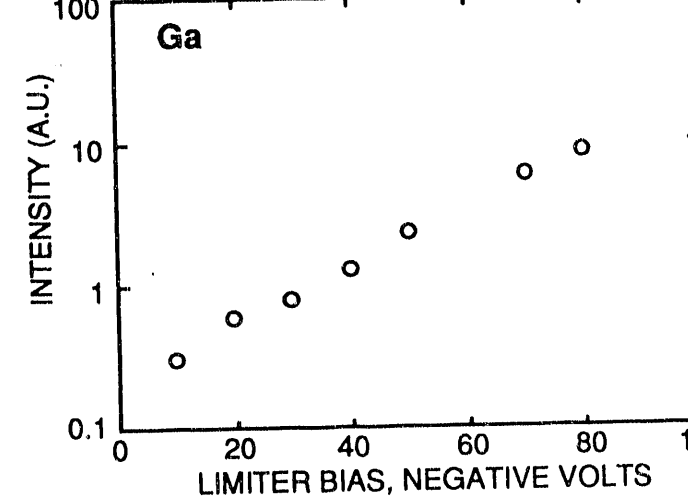
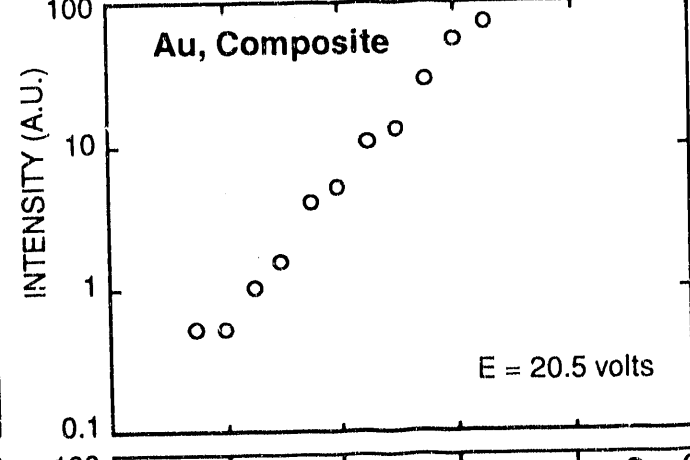
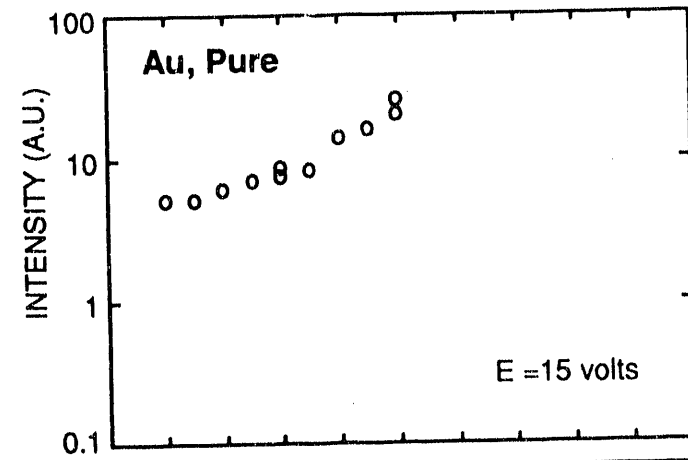
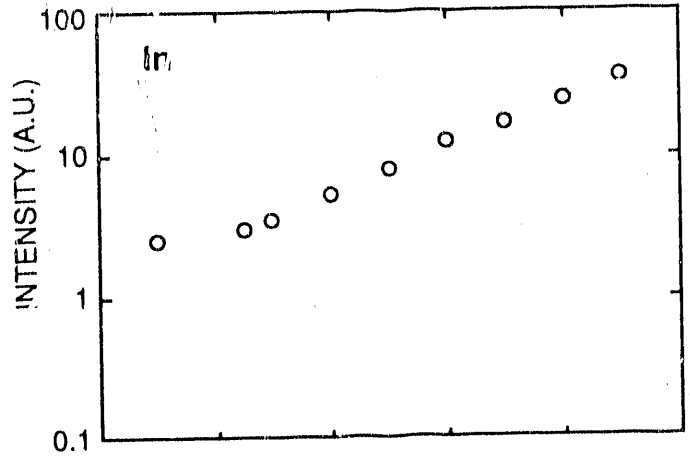
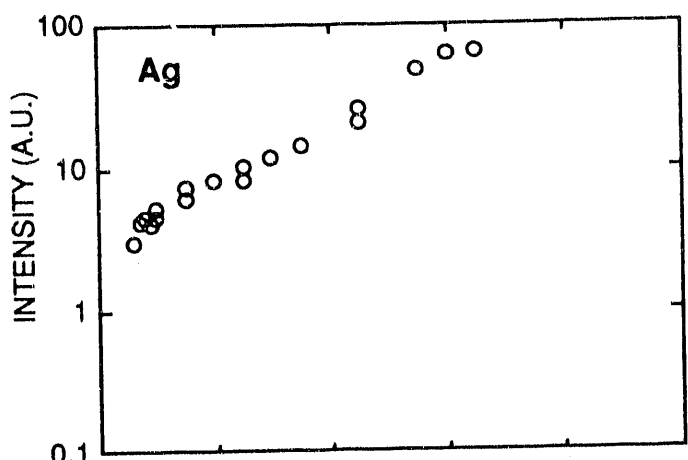




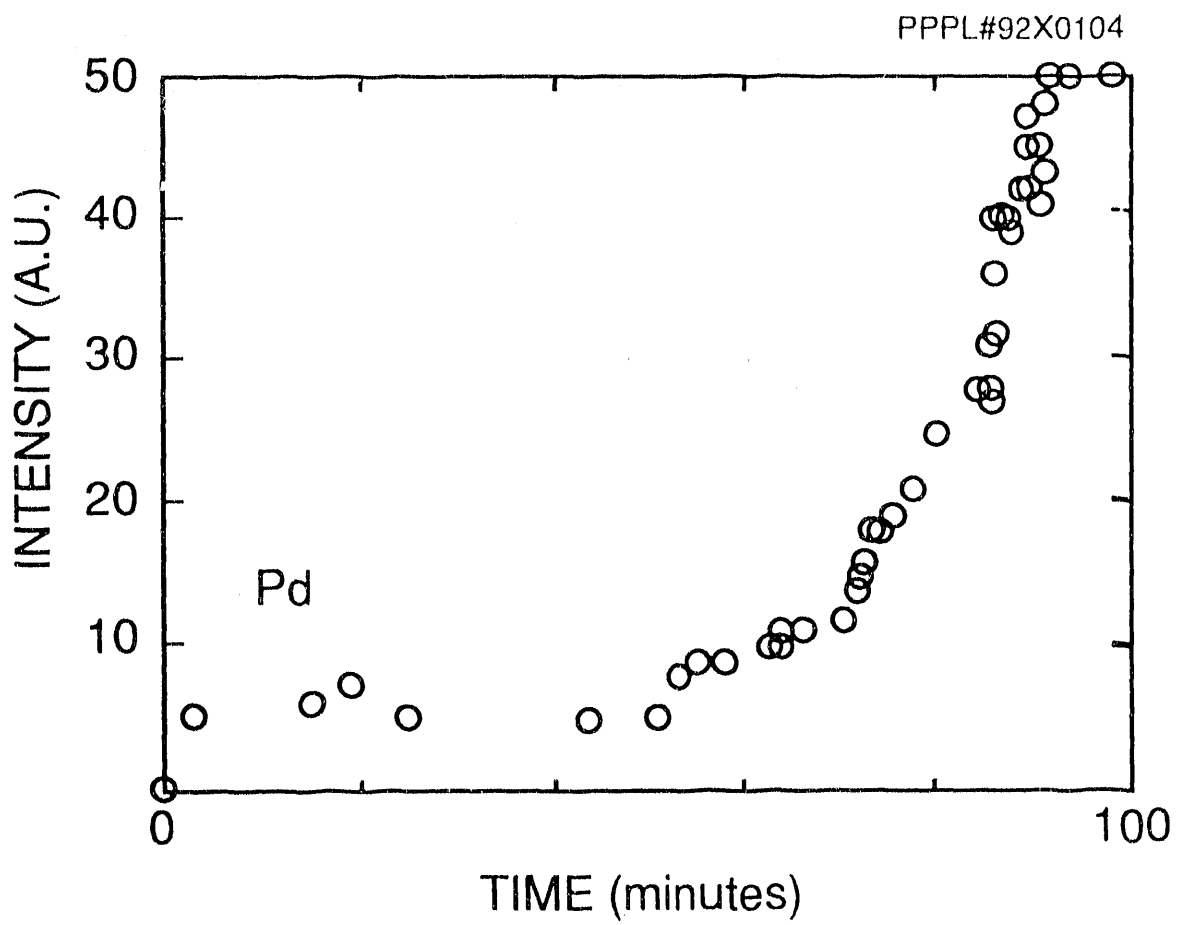
Manos et al  
10<sup>th</sup> PSI  
Fig 4



Manos et al  
10<sup>th</sup> PSI  
FIG 5



Manos et al  
10<sup>12</sup> PaI  
FIG 6



Manos et al  
10<sup>th</sup> PSI  
FIG. 7

**END**

---

**DATE  
FILMED**

**6 / 22 / 92**

